Pitch angle distribution in solar energetic particle events

Author: Arnau Martorell i Rovira
Advisor: Maria dels Àngels Aran Sensat
Facultat de Física, Universitat de Barcelona, Diagonal 645, 08028 Barcelona, Spain.*

Abstract: The transport of solar energetic particles (SEPs) in the interplanetary space is mainly described by the competition between two processes: adiabatic focusing and pitch-angle scattering off irregularities of the mean large-scale interplanetary magnetic field. The purpose of this work is the analysis of the particle directional intensities measured during 2011 November 3 and 2010 August 14 SEP events in order to extract information of the transport processes undergone by the particles. This work involves the use of in-situ particle and solar wind plasma measurements from the Wind spacecraft.

I. INTRODUCTION

Solar energetic particle (SEP) events can be observed in the Earth's orbit. These particles are electrons, protons and other heavier ions with kinetic energies ranging from ~10 keV/nuc to ~1 GeV/nuc. By analysing these SEP events, information about their parent solar activity can be inferred as well as about the solar interplanetary magnetic field (IMF). SEP events are usually classified into impulsive or gradual events according to their characteristics (see e.g., Reames et al. 1999) [1]. Impulsive events are commonly associated with solar flares and are usually characterized by an impulsive increase and a shorter decay of the particle intensity-time profiles and typically last < 24 hours. On the other hand, gradual events are associated with shock waves generated by coronal mass ejections (CMEs) and reach higher intensity levels than impulsive events and may last several days.

Once a SEP escapes from its acceleration site (a flare or a CME-driven shock), it propagates along the IMF into the interplanetary space. The large-scale configuration of the IMF follows the shape of an Archimedean spiral and the magnetic field strength, **B**, decreases with the heliocentric distance from the Sun (see, e.g., Aran et al. 2018, and references therein) [2].

The motion of a charged particle immersed into the IMF can be treated as the superposition of a fast circular motion around a point, called guiding center (GC), the motion of this GC parallel to the IMF and a relatively slow drift of this point. The gyration of the particle becomes of less importance if we follow its motion for a long time (it can be averaged out), and hence the particle's motion in described by the motion of this GC and the particle is always within a gyroradius from it.

Up to a first-order approximation, one can assume that the IMF weakly varies on a scale compared with the distance travelled along the field by a particle over one gyration. Under such assumption, the magnetic moment of the particle associated with its gyration, |**m**| is conserved, being |**m**| named the first adiabatic invariant. The magnetic moment is given by

$$|m| = \frac{\frac{1}{2}mv_{\perp}^2}{B} = \frac{W_{\perp}}{B} \qquad (1)$$

Where $W_{\perp}$ is the kinetic energy associated with the perpendicular component of the particle's velocity $\vec{v}$ to the magnetic field.

The pitch angle (PA) α is the angle between the velocity vector of a particle and the local magnetic field. Usually we use the cosine of the PA, named μ, to study the particle distribution during a solar event. In this case we have that

$$|m| = \frac{\frac{1}{2}mv_{\perp}^2}{B} = \frac{\frac{1}{2}mv^2(1-\mu^2)}{B} = \frac{W_{\perp}}{B} \qquad (2)$$

When a particle is moving into a diverging magnetic field such as the IMF, its $W_{\perp}$ decreases while $W_{\parallel}$ increases to keep W and $|m|$ constant. This causes the adiabatic focusing effect leading the particles to decrease their PA and slowly aligning with the magnetic field lines.

The smooth large-scale configuration of the IMF is perturbed by small-scale irregularities. These irregularities affect the transport of the particles and can be treated, in a first-order approximation, as a pitch-angle scattering process. This scattering effect counteracts the effect of the adiabatic focusing, and tends to increase, in average, the particle's pitch angle (e.g., Ruffolo et al. 1995) [3].

II. EXPERIMENTAL DATA

The data that has been used in this project [4] comes from the Wind spacecraft which is a spin stabilized spacecraft from NASA and orbits the Sun at the L_1 Lagrangian point of the Sun-Earth system. 92s averaged data of solar wind velocity, density, magnetic field provided by the Solar Wind Experiment, Wind/SWE (Olgivie et al., 1995) [5] were used alongside with data from 50-82 keV electron intensities for different PAs from the Three-Dimensional plasma and energetic Particle investigation (Wind/3DP) instrument (Lin et al., 1995) [5]. to determine the pitch angle distribution (PAD) of the two studied events.

The 50-82 keV energy channel was chosen from the one hand because electrons within this energy window have sufficient energy to be clearly distinguished from the electron plasma and suprathermal populations, and hence they are not much affected by local changes of the IMF and from the other hand because their particle intensities show a significant enhancement above background intensity levels.

The electron data provided by the Wind/3DP instrument team [6] has a variable temporal resolution of approximately 24 seconds, but this time lapse can fluctuate between measurements. Electron intensities are given separately in eight different PAs for the electrons reaching the detector. These eight PAs fluctuate over time (as magnetic field direction does) but can be described by their average value. These values of the PA are $\alpha \approx 13°$, $\alpha \approx 34°$, $\alpha \approx 57°$, $\alpha \approx 79°$, $\alpha \approx 101°$, $\alpha \approx 123°$, $\alpha \approx 145°$, $\alpha \approx 162°$.

Remote-sensing data catalogues were also consulted to determine the solar activity that generated the SEP events. The SOHO/LASCO CME catalogue [7] was used to identify the time of occurrence and characteristics of both flares and

* Electronic address: arnaumra@gmail.com

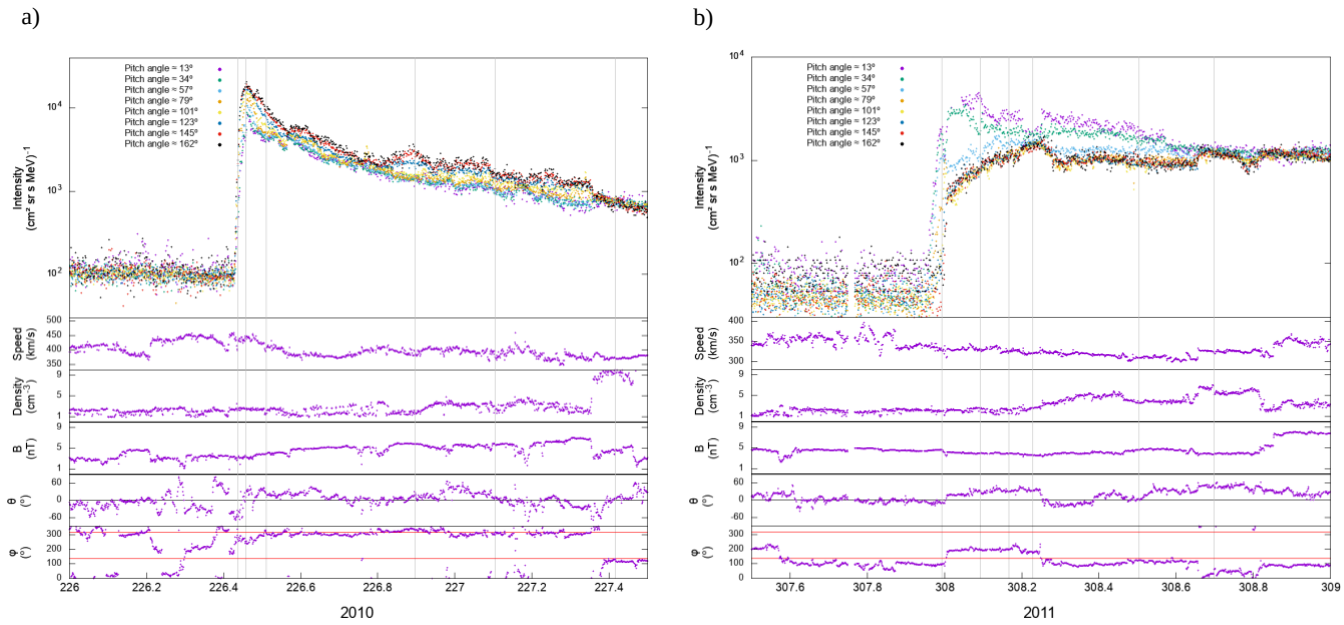

FIG. 1: Wind SEP, plasma and magnetic field observations. From top to bottom, intensity-time profiles for 50-82 keV electrons reaching the detector with different Pas (colour coded), solar wind proton speed and density, magnetic field magnitude, latitude and azimuthal angles. The left panel corresponds to the 2010 August 14 event and the right panel to the 2011 November 3 event.

CMEs, that we use later to calculate the electron travel time from Sun to 1 AU. This CME catalog is generated and maintained at the CDAW Data Center by NASA and The Catholic University of America in cooperation with the Naval Research Laboratory. SOHO is a project of international cooperation between ESA and NASA. The X-ray database from the Geostationary Operational Environmental Satellite (GOES) [8] was used to identify the flare location in the solar disk, start and maximum peak time when it was not provided by the SOHO/LASCO CME catalogue.

III. DATA ANALYSIS AND RESULTS

Prior to study the SEP events, electron intensity data was averaged over two and a half minutes time periods to reduce the noisy fluctuations exhibited by the provided particle data set. Note that detection-uncertainties are not provided by the instrument team, and therefore, we have not taken them into account.

Subsequently, particle and plasma data was plotted to analyse the SEP events, and after that, some time snapshots were taken to study the PADs in different phases of the particle events.

Finally, the SOHO LASCO CME catalogue was consulted to determine the solar source of the electron events and to calculate the time used by the electrons to reach 1AU and compare it with a time calculation done approximating the IMF by an Archimedean spiral (named Parker spiral after Parker, 1958) [9].

A. SEP event analysis

Fig. 1 shows a summary of in-situ particle, plasma and magnetic field observations from Wind. Each panel shows from top to bottom: angular particle intensities for 50-82 keV electrons (PAs are assigned to different colours and indicated in the legend), solar wind proton speed and density and magnetic field data, magnitude (strength), latitude and azimuth angle in the Geocentric Solar Ecliptic (GSE) coordinate system, as a function of time. Time is given in Days Of Year (DOY). In the GSE coordinate system, the X-axis points towards the Sun, the Z-axis to the North Ecliptic pole and the Y-axis completes the right-handed triad

Fig. 1a shows data from 2010 August 14 (day 226 of year) to August 15 (day 227 of year) and Fig. 1b from 2011 November 3 (day 307 of year) to November 5 (day 309 of year). Vertical grey lines in Fig. 1 shows the times for the analysed PADs (more details on section III.B).

In Fig. 1a one can see from the IMF azimuthal angle that the solar magnetic field was pointing towards the Sun during the major part of the event, but before the onset of the electron intensities it suffered a rotation indicated by a simultaneous change in the latitudinal and azimuthal angles. The polarity of the IMF is reversed towards the end of the plotted period, as indicated by a sudden change in the azimuthal angle, suggesting that the spacecraft entered into a different IMF sector.

From the intensity-time profiles one can see that during all the event the electron intensity was nearly the same for all PAs which means that electrons suffered significant scattering processes during their transport from the solar source to the spacecraft, and that leads to isotropisation of the intensities in the decaying phase, especially after the sector change. The increment of the anisotropy of the angular intensities seen the end of August 14 will also be discussed in section III.C.

In Fig. 1b one can see from the azimuthal angle that the magnetic field was pointing outwards from the Sun during the whole event, but it has to be noticed that during the prompt phase, a change of magnetic field flux tube occurred from DOY 208-208.25. Furthermore, at the end of November 4, a smooth rotation of the IMF starts simultaneously with a sudden increase of the magnetic field strength and solar wind speed, followed with a soft decrease of both magnitudes until ~14 UT on DOY 309 (not shown here). This suggests the presence of a magnetic structure like an interplanetary CME, that may

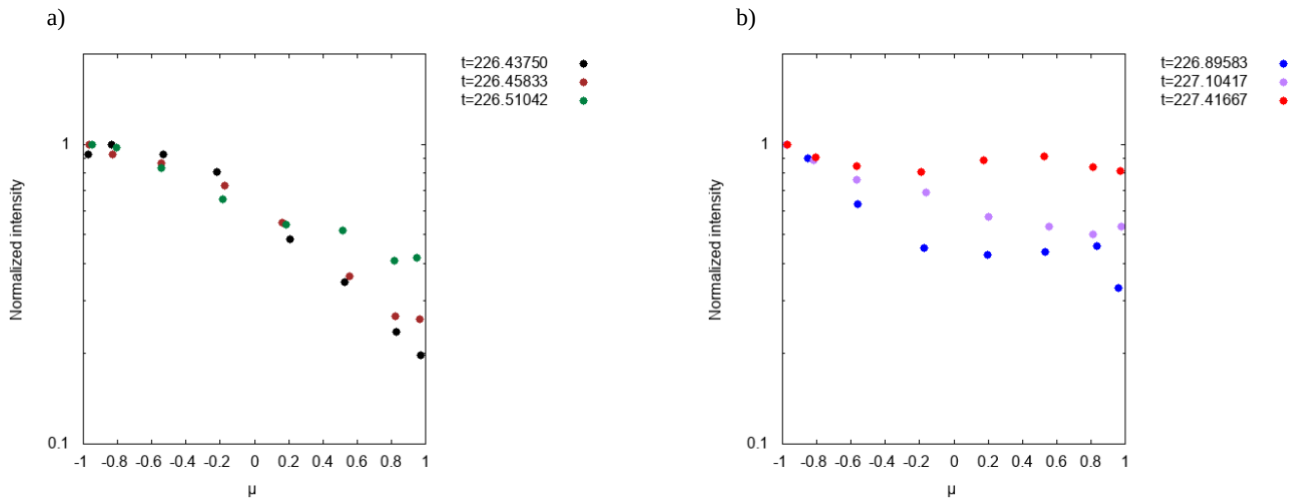

FIG. 2: Normalized intensity as a function of μ for the August 2010 event. Fig. 2a shows the first three snapshots while Fig. 2b shows the three final ones.

have left the Sun the previous days. This solar wind feature does not affect the angular distribution of the particles significantly. Electron angular intensities show similar values from the afternoon of DOY 308.

It also has to be mentioned that during this event, the latitudinal angle of the magnetic field remains much closer to the ecliptic plane than during the August 2010 event which means that the IMF remains close to the ecliptic. This together with the fact that the azimuthal angle keeps roughly constant around 135º, the assumption of a Parker spiral IMF is rather accurate for this event.

From the electron intensity-time profiles it is easy to notice that the intensity peak is higher for the smallest PA, which means that there are more electrons coming well aligned with the magnetic field than those that are not. This alignment shows that focusing processes were more important during the transport from the sun to 1 AU
than the scattering processes during the prompt phase of the event.

While in Fig. 1a it is clear that the onset is the same for all the PA, in Fig. 1b we can see that there is a time delay between the onset in particles coming in the direction of the field and those coming in the opposite direction which further indicates that scattering processes were more important in the case of the 2010 August 14 event than for the 2011 November 3 event.

B. Pitch angle distributions

Fig. 2 and Fig. 3 show the PADs for selected times in the events. To obtain the PADs we have normalized the angular intensities to the maximum value measured across pitch angles. Hence these figures show the normalized intensity as a function of μ. Fig. 2 correspond to the August 2010 event while Fig. 3 corresponds to the November 2011 event. Plotted times in Fig. 2 are those marked by a vertical grey line in Fig. 1a, while the times in Fig. 4 correspond to those in Fig. 1b.

In a PADs plot, the isotropy of the electron distribution is indicated by the flatness of the normalized intensity profile. The flatter profile for the different PA, the more isotropized the electron distribution. Fig. 2a shows that at the rising phase of the event (black dots) the highest anisotropy is observed. Note that the maximum intensity corresponds to the PAs of the electrons better aligned with the field (those with $\mu \approx -1$ since the magnetic field is pointing towards the sun while the electrons move outwards). We can see that they seem to have a flat profile, but this profile rapidly loses its flatness for higher values of μ. This profile matches with the idea than when the event starts, we have the higher intensity in the direction of the field but, in the opposite directions, we will still have to wait some time to see intensities similar to those in the magnetic field directions. During the peak and shortly after it (brown and green dots respectively) we see that the anisotropy slowly decreases leading to a flatter profile for later times.

Looking at Fig. 1a one can see that if we had plotted the PAD for a time after the peak but before the secondary peak in later August 14, we would have obtained a flatter PAD-profile than those commented so far. Contrary to this, we see in Fig. 2b, during this secondary peak (blue dots), that the difference in intensity between the well ($\mu \sim -1$) and worse ($\mu \sim 1$) aligned electrons is larger than for the previous time. This behaviour suggests a new injection of electrons. We will discuss this in section III.C.

After that, we can see that isotropy is slowly recovered (purple dots) and finally, after one day from the onset (red dots) we have the electron distribution well isotropized. It is reasonably to think that the isotropization near DOY 227.4 is due to the change of polarity of the IMF.

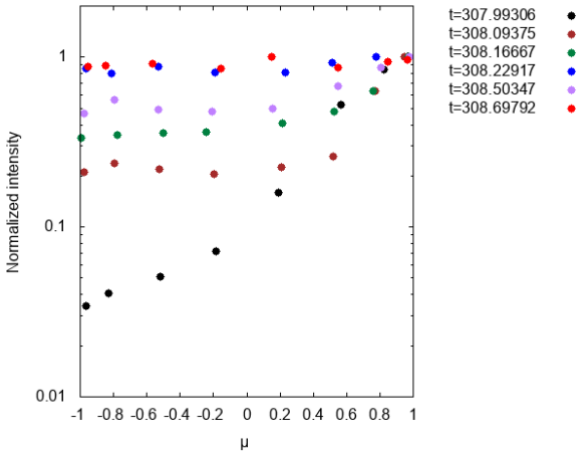

FIG. 3: Normalized intensity as a function of μ for the November 2011 event.

In Fig. 3 the first thing we can notice is that the maximum intensities correspond to higher values of μ, that happens because contrary to the case in the August 2010 event, the IMF is pointing outwards from the Sun, so since electrons are moving in the same direction, we found the higher intensities in that angular window.

During the onset of this event (black dots) there is a clear anisotropy of the electron distribution due to the time delay for the different PAs mentioned in section III.A, this is indicated by the steep slope in Fig. 3. During the peak (brown dots) it is easy to see from Fig. 1b that the two lowest PA follow a different profile than the one presented by the others, this produces that in Fig. 3 the first six PA seem to have a flat profile, meaning that the electron distribution is almost the same in those directions, but there is a huge difference between the PAs corresponding to electrons following the magnetic field direction and the other six PAs. This tendency continues shortly after the peak (green dots). This feature together with the different onset times are an indication that the scattering processes suffered by the electrons in this event are weaker than for the August 2010 event.

Near the DOY 308.2 all the intensity profiles in Fig. 1b show similar values for a small time interval. That is the reason why in Fig. 3, for that time snapshot (blue dots), the profile seems almost completely flat. The reason for this behavior is unclear. Later, we can see that isotropy is slowly recovered (purple dots) until finally a flat profile (red dots) is obtained at the moment where the magnetic field gets close to the polarity reversal.

C. Solar sources

According to W. Dröge et al. [10] the 2010 August 14 event started with a solar flare at ~N17W52 around 9:40 UT. Thus, the Wind spacecraft is well-connected to the flare site through the IMF. This flare was accompanied by a coronal and interplanetary type II radio burst starting at 9:52 UT, which indicates the presence of a shock wave. This shock wave wave affected the escape of the electrons towards the interplanetary space [10] and might help explaining the relatively low anisotropy observed for this event, since the presence of a shock may have disturbed the IMF close to the Sun, making the scattering processes more relevant than the focusing ones.

According to R. Gómez-Herrero et al. [11] the 2011 November 3 event was related to several flares at ~N20E62 with an X-ray flare peak at 22:41 UT producing the electron injection. This means that the Wind spacecraft had a priori poor magnetic connection with the parent solar activity originating the electron event. This might indicate delayed onset times for the particle intensities observed by Wind.

As mentioned before, the anisotropy increase seen at the secondary peak in the 14 August 2010 event might be related to a new injection of particles from another solar source. We have check for this possibility. The X-ray flare catalogue from the Geostationary Operational Environmental Satellite (GOES) [8] was consulted in addition to the SOHO/LASCO CME catalogue [7] to determine if this secondary peak was caused by another smaller event. From the CME catalogue two narrow and slow CMEs started between 14:00 UT and 16:00 UT lasting only a few minutes, that cannot explain the acceleration of new SEPs. However, the X-ray catalogue and the CME catalogue indicate occurrence of a new X-ray flare starting at 18:03 UT, from the same active region of the flare originating the particle event. Taking into account that the time spent by the electrons to reach the peak value since they were released from the Sun is of about 1 hour 20 minutes, electrons injected during this flare would reach Wind at about 19:39 UT. This time matches with the time at which the secondary peak appears in the intensity profile on Fig. 1a. Therefore, this secondary peak may be attributed to the electrons arriving from this second solar flare.

D. Travel times

According to the flare start time and the times for electron intensity onsets, the time spend by electrons travelling from the Sun to Wind was about 40 minutes for the 2010 August 14 event and about 25 minutes for the 2011 November 3 event. For this later event, it has been used the onset time of the well-aligned electrons (the lowest PA) for which the onset occurs earlier than for the other PAs.

The fact that the observed travel time is longer for the August 2010 event is in agreement with the information provided by the PADs regarding the importance of the PA scattering processes in this event, that may have delayed the onset of the particle intensities. In addition this delayed onset may also be explained by the presence of a shock wave that may have prevented the fast escape of the electrons from the Sun [10] as well as it might have contributed to disturb the electrons journey from the Sun to Wind, as mentioned in section III.C.

Approximating the solar magnetic field by the Parker spiral, a perfect spiral in the ecliptic plane, we can estimate the distance travelled by the electrons. The speed of the electrons can be obtained from their kinetic energy by using

$$E_c = (\gamma - 1)mc^2 \qquad (3)$$

where m is the mass at rest and γ is the Lorentz factor. Knowing the speed and the distance travelled, we can estimate the time at which the intensity onset of these two events would occur if the magnetic field was not disturbed and the particle travelled in scatter-free conditions.

From Equation (3) we obtain: $V_{50\ keV} \approx 0.41c$, $V_{65\ keV} \approx 0.46c$, $V_{82\ keV} \approx 0.5c$

To estimate the path length along the Parker spiral we use

$$s = \frac{1}{2}\frac{u_{sw}}{\omega_\odot}\left(\psi \cdot \sqrt{\psi^2+1} + \ln\left\{\psi + \sqrt{\psi^2+1}\right\}\right) \qquad (4)$$

Where u_{sw} is the solar wind velocity averaged for the whole event duration, $\omega_\odot$ is the solar angular velocity and $\psi = \omega_\odot r/u_{sw}$ being r the distance between one solar radius and 0.99 AU (Wind's distance from the Sun). Equation (4) leads to $s = 1.7489 \cdot 10^{11}\ m$ for the 2010 August event, and $s = 1.8441 \cdot 10^{11}\ m$ for the 2011 November event.

TABLE I: Results from the approximated electron travel time calculation for a Parker IMF configuration.

2010 August 14 SEP event	$t_{50\ keV} \approx 25.56\ min$
	$t_{65\ keV} \approx 21.09 min$
	$t_{82\ keV} \approx 19.16\ min$
2011 November 3 SEP event	$t_{50\ keV} \approx 24.84\ min$
	$t_{65\ keV} \approx 22.21\ min$
	$t_{82\ keV} \approx 20.20\ min$

Table I shows the estimated electron travel times for both events calculated from the obtained path lengths and particle speeds. Comparing this approximated electron travel times with the ones measured from data, it is easy to see that the Parker spiral approximation is pretty good for the 2011 event while it does not really match with the 2010 event.

The reasons for the mismatch in the case of the August 2010 event have been already studied at the beginning of this section. On the other hand, in the case of the 2011 November 3 event, the agreement could be explained by the good approximation of the observed IMF with a Parker field throughout the event. However, the Wind spacecraft had a poor magnetic connection with the flare site, in this event, which is at odds with the observed particle onset. Gómez-Herrero et al. [11] indicate that the magnetic field was largely disturbed in the solar corona November 2011, enabling a direct magnetic connection between the Earth and the Sun.

Also note that the R. Gómez-Herrero et al. [11] determined that the value of the particle mean free path that best fits this event is of 0.7 AU, which supports our conclusions drawn from the analysis of the PADs and of the travel and onset times, that indicated the predominance of the focusing effect over the pitch-angle scattering processes. On the other hand, Dröge et al. [10] obtained a mean free path of 0.2 AU for the 2010 event, consistent with a turbulent IMF (possibly due to a shock wave). This can explain the difference between measured and calculated travel times as an electron during this event may have suffered of the order of 5 scattering processes before reaching the detector.

IV. CONCLUSIONS

- The study of the PAD allowed us to identify if during the electron transport scattering processes had relevance or were the focusing processes the most relevant instead. As shown in section III.D, during the 2010 event scattering processes were the ones governing, however, during the 2011 event focusing was the dominant effect, leading to a great difference in the intensity profiles for the different PA as shown in Fig. 1b.

- We detected an anomalous behaviour in the PAD during the 2010 event that has led us to determine a second SEP event, a few hours after the main one, producing this strange behaviour in the intensity profile and the PAD.

- The estimated electron travel times allow us to confirm that the solar sources named in section III.B as the main sources of the two SEP events analysed in this work.

Acknowledgments

We acknowledge the use of publicly available data products from Wind /SWE and 3DP. We acknowledge the use of the X-ray database from GOES and the CME catalogue from SOHO/LASCO. Thanks my advisor, Dr. A. Aran for her guidance and help during this remotely supervised TFG. Thanks to my family for their patience and support.

[1] Reames, D.V. «Particle acceleration at the Sun and in the heliosphere». *Space Science Reviews* **90**, 413–491 (1999). https://doi.org/10.1023/A:1005105831781

[2] A. Aran et al. «Charged particle transport in the interplanetary mediu», O.E. Malandraki, N.B. Crosby (eds.), «Solar Particle Radiation Storms Forecasting and Analysis, The HESPERIA HORIZON 2020 Project and Beyond», Astrophysics and Space Science Library 444, DOI 10.1007/978-3-319-60051-2_4

[3] Ruffolo, D.. (1995). «Effect of Adiabatic Deceleration on the Focused Transport of Solar Cosmic Rays». The Astrophysical Journal. 442. 861. 10.1086/175489.

[4] NASA 2014, *Index of /wind3dp/data/wi/3dp*, Wind 3-D Plasma and Energetic Particle Investigation Home Page, viewed May 2020, http://sprg.ssl.berkeley.edu/wind3dp/data/wi/3dp/

[5] Ogilvie, K.W., Chornay, D.J., Fritzenreiter, R.J. et al. SWE, a comprehensive plasma instrument for the WIND spacecraft. *Space Sci Rev* 71, 55–77 (1995). https://doi.org/10.1007/BF00751326

[6] Lin, R.P. et al., «A Three-Dimensional Plasma and Energetic Particle Investigation for the Wind Spacecraft», Space Science Reviews, 71, Issue 1-4, 125-153 (1995).

[7] NASA 2010, SOHO LASCO CME catalogue, NASA, viewed June 2020, https://cdaw.gsfc.nasa.gov/CME_list/

[8] NOAA, National Centers for environmental information, viewed June 2020 ftp://ftp.ngdc.noaa.gov/STP/space-weather/solar-data/solar-features/solar-flares/x-rays/goes/

[9] Parker, E.N., « Dynamics of the interplanetary gas and magnetic fields», *Astrophysical J.*, 128, pp 664-676, (1958)

[10] W.Dröge et al, «Multi-spacecraft observations and transport modeling of energetic electrons for a series of solar particle events in august 2010» *The Astrophysical Journal*, vol. 826, pp. 17-34, 2016.

[11] R.Gómez-Herrero et al, «Circumsolar energetic particle distribution on 2011 November 3», *The Astrophysical Journal*, vol. 799, pp. 17-34, 2015.